Metallurgical and Materials Engineering *Research paper*
Association of Metallurgical Engineers of Serbia AMES *https://doi.org/10.30544/571*

EFFECT OF PROCESS PARAMETERS ON THE PHASE TRANSFORMATION KINETICS IN COPPER-BASED ALLOYS AND COMPOSITES

Marko Simić[1], Nenad Radović[2], Milan Gordić[1], Jovana Ružić[1]*

[1]Department of Materials, „VINČA" Institute of Nuclear Sciences - National Institute of the Republic of Serbia, University of Belgrade, PO Box 522, 11001 Belgrade, Serbia
[2] Faculty of Technology and Metallurgy, University of Belgrade, Karnegijeva 4, 11120 Belgrade, Serbia

Received 08.10.2020
Accepted 02.11.2020

Abstract

Copper-based alloys and composites, owing to their convenient properties, are being considered essential materials in various industries. Since copper possesses an ability to develop high corrosion resistance, putting it in the domain of a desirable material in the manufacturing of valves, pipes, and also systems that carry industrial gases and aqueous fluids. Its usage is also invaluable for cables and electrical wires. This review paper describes diversity in copper alloy processing techniques (powder and ingot metallurgy) which are alongside the phase transformation kinetics interpreted and explained in detail. Furthermore, the focus is put on the copper alloys, as well as the kinetics present in these systems, with the application being highlighted. Correlation between physical properties and phase transformation kinetics in copper alloys is made. It is shown that if certain alloying elements are to be added, different properties could be improved. The effect of phase precipitation on phase transformation kinetics of copper alloys is shown by studying the Cu–15Ni–8Sn alloy.

Keywords: copper**;** copper alloys; phase transformation kinetics; process parameters.

Introduction

Copper and copper alloys are widely used in our modern everyday life. Owing to their properties, they have a major role concerning automotive radiators, home heating systems, heat exchangers, solar collectors, and numerous other systems where rapid conduction of heat across or along a metal section is a requirement [1-3]. When parts must conduct electrical current, then pure copper is normally used, usually as electrical

*Corresponding author: Marko Simić, *marko.simic@vin.bg.ac.rs*

wires and cables. Having the ability to withstand corrosion, coppers, bronzes, brasses, and copper nickels have found use in pipes, valves, and systems carrying aqueous fluids and industrial gases [1]. Before discussing different copper alloy and composite families, a distinction between the two is in order. Although they may seem similar at first glance as they both consist of at least two components, taking a deeper look will set them apart. While an alloy is a mixture of a minimum of two elements where at least one must be a metal, on the other hand, composite material does not require metal to be included in the mixture. Copper alloys are identified by the Unified Numbering System (UNS), which categorizes families of alloys based upon their composition [1]. UNS designations for different alloys are shown in Table 1. The following Table 2. shows mechanical and physical properties, such as hardness, strength, the electrical and thermal conductivity of the copper and related selected elements [4-6]. Having seen parameters related to relevant conductivity, as shown in Table 2., thermal and electrical conductivity parameters can also be distinguished between different copper alloys as well, as shown in Fig. 1.

Table 1. UNS copper alloy designations, wrought products are assigned numbers between UNS C10000 through UNS C79999, and cast products range from UNS C80000 to UNS C99999 [1].

Alloy	*Wrought*	*Cast*
Copper	C10100 to C13000	C80100 to C81200
Brass	C20500 to C28580	C83300 to C85800
Tin Brass	C40400 to C48600	C83300 to C85800
Phosphor Bronze	C50100 to C52400	C90200 to C91700
Aluminum Bronze	C60800 to C64210	C95200 to C95900
Silicon Bronze	C64700 to C66100	C87000 to C87999
Silicon Red Brass	C69400 to C69710	C87300 to C87900
Copper Nickel	C70100 to C72950	C96200 to C96900
Nickel Brass	C73500 to C79900	C97300 to C97800

Table 2. Mechanical and physical properties of copper and selected elements [4-6].

Metal	*Hardness (HV, MPa)*	*Strength (MPa)*	*Relative electrical conductivity (%)*	*Relative thermal conductivity (%)*
Silver	25-27	125	106	108
Copper	50	210	100	100
Aluminum	26	90	62	56
Iron	150	180-210	17	17
Lead	5	18	8	9

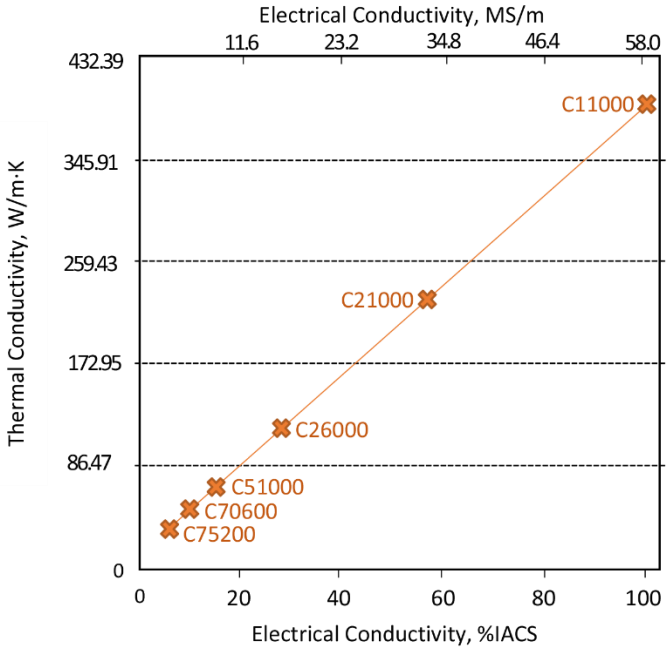

Fig. 1. The relationship between thermal and electrical conductivity for selected copper alloys, indicated in Table 1 [1].

As already mentioned, in the past couple of years, improved copper-based alloys have been estimated as possible materials for applications in various industries, ranging from automotive and aerospace to electrical [7]. With proper processing techniques, it is even possible to create such mechanical properties that can combat harsh conditions in industries such as the rocket industry or nuclear technology [8, 9]. In this review paper, techniques for material processing are discussed and explained, with them being powder metallurgy (PM) and ingot metallurgy. Powder metallurgy consists of two main steps: (i) forming of the powder mixture (using milling or mixing), (ii) densification of the powder mixture (cold or hot pressing, sintering, extrusion, forging, etc.). On the other hand, ingot metallurgy is high-temperature processing of metals, which is based on the metal casting process, which means pouring metal in a liquid state (metal at a temperature above its liquidus temperature) in a mold for cooling. In recent decades, casting processes that operate with metals in a semi-solid state (compo casting, rheo casting, and thixo casting) are being actively in use [10].

In the early 1990s, a new technique that involved the utilization of laser for material synthesis by means of powders consolidation was starting to develop [11]. This technique takes primacy over other techniques when versatility, flexibility, time and energy economy, and faster heating and cooling rate are considered. The essence of the laser sintering technique lies in the *in situ* exothermal reactions between the elements or between an element and a compound within a metal matrix, where the fine and thermodynamically stable ceramic phases are formed. Reaction processes between the structural components in obtaining particle reinforcement can occur in both the solid and liquid state [11-15]. The *in situ* metal-based composites exhibit enhanced wear

resistance and improved mechanical properties such as strength and hardness [16]. Due to the lack of flexibility to control the *in situ* reaction process in the liquid metallurgy process as well as the often-present rough crystal grain of the metallic matrix and complex interface structure, a new method was developed [17]. The hot-pressed sintering method can undisputedly produce high-density materials and avoid the before mentioned limitations of the liquid metallurgy route [18].

Further development of different techniques has led to the powder metallurgy method, which is a combination of mechanical alloying and hot-pressing process. There are many advantages of incorporation of a hard-ceramic material such as ZrB_2 to the Cu matrix as they can notably enhance wear and spark resistance and mechanical properties. Another significant advantage is the perseverance of high electrical and thermal conductivity of Cu based composites [19,20]. Particles of Zr and B are mechanically activated during the mechanical alloying, and that permits *in situ* forming of nano and micro ZrB_2 reinforcing particles in the copper matrix in the course of the hot-pressing process [20]. From the casting point of view, compo casting could be used to produce metal-based composites with particulate reinforcements where reinforcing particles are inserted in the semi-solid metal matrix during mixing. Hence, copper-based composites reinforced with micro ZrB_2 particles are obtainable using the casting process followed by heat treatment [21].

Phase transformation kinetics

There are multiple methods for the determination of phase diagrams. The one described in Fig 2. focuses on property changes during cooling and/or heating of an alloy, which can be thermal, mechanical, chemical, or physical, and through this, approaches a system to the equilibrium state. The other group of methods, unlike the first, employs equilibrated alloys, which means that it emphasizes the behavior of a system in equilibrium or local equilibrium state [22].

The two approaches for the determination of phase diagrams are schematically illustrated in Fig. 2. Observing the phase diagram (Fig. 2b), it becomes evident that with the slow cooling to the Ts temperature, in an alloy with composition X_2, the α phase starts to form. Since the properties of the α phase differentiate from those of the γ phase, then by observing the variance of a specific property (electrical conductivity) with temperature, it becomes possible to estimate the two all-important temperatures Ts and Tf (transformation-start and transformation-finish temperatures). This assessment is based upon the location of the temperatures, where different curves manifest a change of slope, as can be seen in Fig. 2c.

Ideally, from a theoretical perspective, Ts and Tf temperatures of a few various alloys can be used to determine the equilibrium phase boundaries. On the other hand, this is only possible when the cooling rate is remarkably meager, and when the phase transformation (γ to α) begins exactly at Ts and finishes at Tf [23]. For a particle with a size that is exceeding a critical value, a certain undercooling is a necessity. Therefore, the actual Ts is commonly moved towards the lower temperatures throughout the cooling process, all to generate the necessary undercooling. The emphasis should be placed on the determination of phase transformation kinetics during cooling and heating, with the aim of properly estimating the equilibrium phase diagrams [23]. In Fig. 2a the lattice parameter vs. composition plot is presented, where the constant lattice parameters in a two-phase alloy is shown. When sharp changes in the plot presented in

Fig. 2a occur, it becomes possible to determine the phase boundaries (Fig. 2b points C and D).

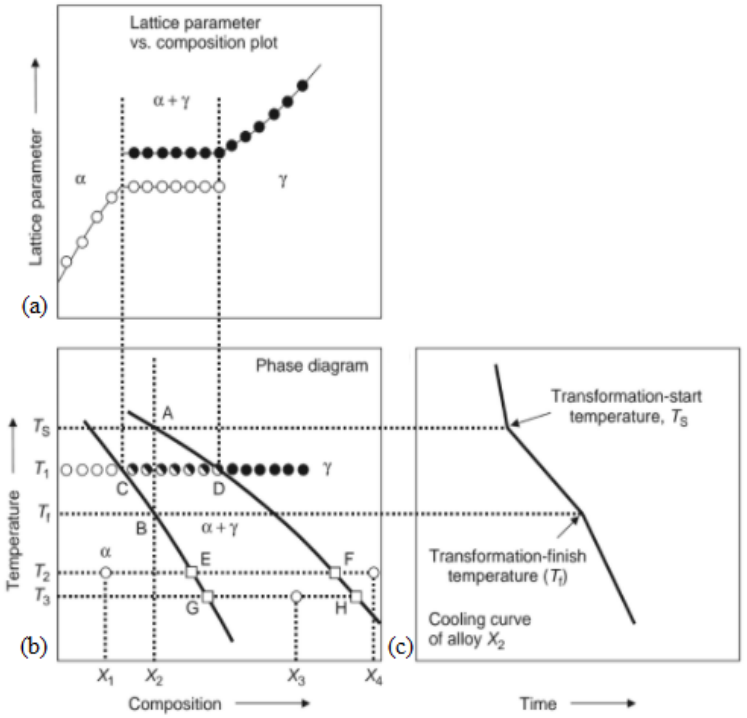

Fig. 2. Schematic diagram showing two approaches for the determination of phase diagrams: (a) schematic plot of lattice parameters vs. composition, (b) schematic phase diagram, and (c) the schematic cooling curve of a specific alloy X_2 [22].

Precipitation of phases from quenched alloys

In most cases time–temperature–transformation (TTT) diagrams are used to depict isothermal phase transformation kinetics [24]. Using these diagrams, it is possible to see when the precipitation starts, as well as when it finishes during the isothermal annealing at different temperatures. If the start times of precipitation are linked together at different temperatures, C-shaped curves, named C-curves, are formed. Fig. 3 presents isothermal decomposition kinetics of Cu–15Ni–8Sn alloy and its relationship with the phase diagram [24]. Fig. 3a shows a vertical section at 15 wt.% Ni of the Cu–Ni–Sn ternary phase diagram. If the diagram is carefully observed, it can be seen that the equilibrium solvus temperature for the above-mentioned alloy is 800 °C. If fast quenching from the temperature of above 800 °C is applied, it is possible to retain the fcc phase up to room temperature. Observing Fig. 3b, it can be noted that due to the isothermal annealing, below the same temperature, different precipitates can be formed in the quenched specimens, depending on the temperature [25].

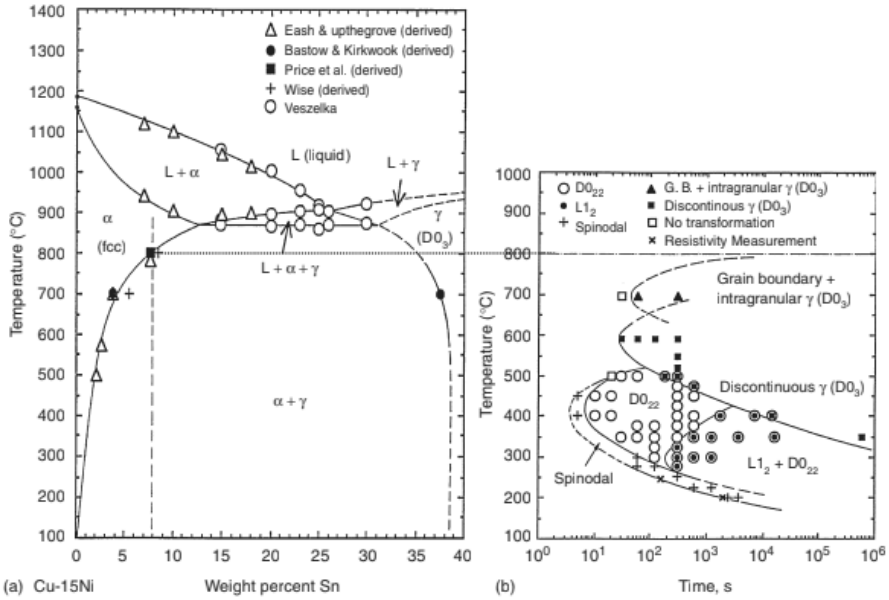

Fig. 3. Isothermal decomposition kinetics of Cu–15Ni–8Sn alloy and its relationship with the phase diagram:(a) isopleth of the Cu–Ni–Sn ternary phase diagram at 15wt.% Sn and (b) TTT diagram of the Cu–15Ni–8Sn alloy [24].

Owing to the relatively fast kinetics of the Cu–15Ni–8Sn alloy, the equilibrium γ (D03) phase is formed relatively easy at temperatures above 500 °C. Beneath this temperature, a much extended time period is necessary for the formation of the equilibrium phase, because the metastable spinodal structure, D_{022}, and L_{12} occur before the equilibrium γ (D03) phase precipitation. Taking this into account, it can be said that more than 300h would be necessary for the formation of the equilibrium γ (D03) phase to start at 300 °C [26]. With the aim to determine the phase equilibrium at 300°C, a quenched specimen should be gradually annealed in small steps. Firstly, the quenched specimens should be annealed at 500 °C for several hours in order to induce the formation of the γ (D03) phase, and afterward, they should be annealed at the temperature of 300 °C with a dwell of extended time period due to reaching the equilibrium at 300 °C.

On the other hand, it is possible to carry out a cold deformation process, taking into account the ductility of the specimen to produce microstructural defects, namely dislocations, in order to ease the formation of the equilibrium phase. The Cu–15Ni–8Sn alloy is an excellent example that can offer a clear understanding and insight into the phenomenon of isothermal precipitation kinetics, providing the reliable phase diagram and hence the phase equilibrium at low temperature [24].

Physical properties in relation with phase transformation kinetics in Cu-Hf alloys

Due to hafnium's promising characteristics and properties, including tremendous resistance to corrosion, it is viewed as a genuinely desirable material in different

superalloys as well as nuclear reactor rods [27]. In the case of copper alloys, the influence of Hf is similar to that of Zr in the sense that it increases the recrystallization temperature and heat resistance of copper. Furthermore, with the addition of Hf, mechanical strength is improved while the electrical conductivity is almost unchanged [28]. Also, it should be mentioned that Cu-Hf alloys possess the precipitation strengthening effect. Furthermore, it can be seen from the binary phase diagram of the Cu-Hf alloy (Fig. 4) that the solubility of hafnium in copper is higher than Zr [29,30]. Namely, the maximum solubility of hafnium in copper at eutectic temperature is 0.4 at.% [29], while that of Zr is 0.12 at.% [30], allowing extra room for additional performance improvements.

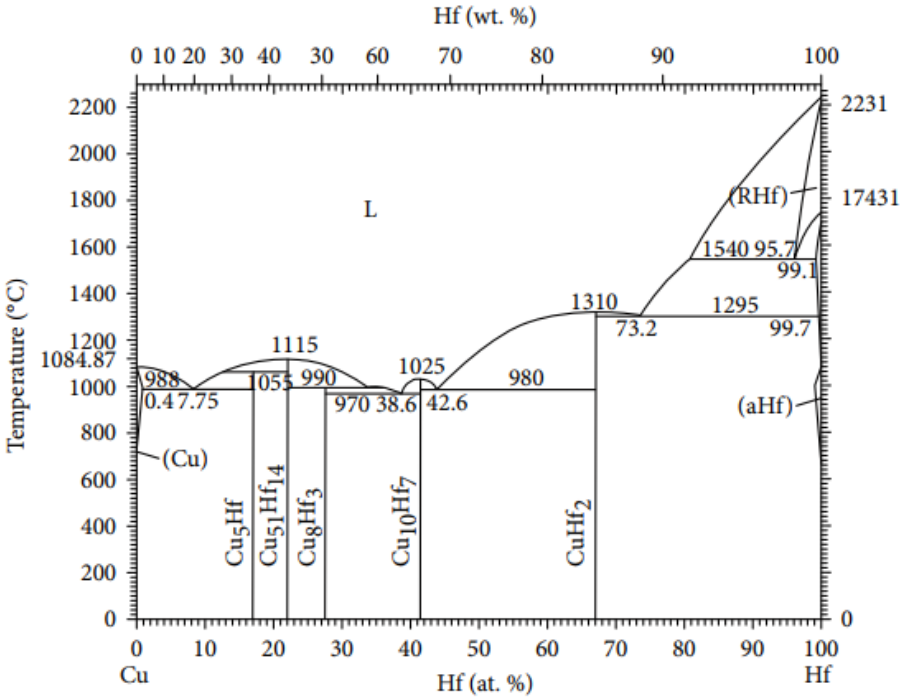

Fig. 4. Binary phase diagram of the Cu-Hf alloy [27].

A group of authors studied and compared copper alloys [27], with three different Hf contents (Cu-0.15Hf, Cu-0.4Hf, and Cu-0.9Hf). Firstly, in the as-cast alloy state, an increase in hardness is noted with the addition of Hf [27]. As can be found in the literature, Cu-0.9Hf has twice the hardness the Cu-0.15Hf alloy has [27-29]. On the other hand, this is not a trend that can be applied to the conductivity, as it decreases with the addition of Hf. When the conductivity of the Cu-0.9Hf alloy is compared with one of the pure coppers, it can be seen that is much smaller. However, it must be noted that variations can be quite large considering the alloy composition. Taking into account the change of conductivity, it does not vary much with the addition of Hf. Following the solid-solution treatment, a vigorous decrease in hardness can be seen, and all due to the grain growth, recrystallization, and the dissolution of the solute into the copper matrix

[29]. It can also be noted that electrical conductivity increases in value as the Hf content decreases. Showing this through an example, the conductivity of Cu-0.4Hf is higher than that of Cu-0.9Hf alloy. Seen through IACS (International annealed copper standard), the conductivity of Cu-0.9Hf is 44.9% IACS, while the conductivity of Cu-0.9Hf is 36.3% IACS [27]. When the alloys are cold rolled, they all exhibit an increase in hardness, however, in this state conductivity does not change much either.

Usually, for the alloys mentioned above, two different aging temperatures are selected, 400 °C and 450 °C with applied dwell up to 90 minutes. For the first two alloys, Cu-0.15Hf and Cu-0.4Hf, an aging temperature of 450 °C is the optimal temperature where the peak aging occurs after 30 minutes, and for the third Cu-0.9Hf, after 60 minutes. After aging, both the values for conductivity and hardness for these alloys are higher than in other possible states, and so it is preferred [27].

Conclusions

In this review paper, contemporary manufacturing processes of a few copper alloys and their composites are outlined. It was shown that techniques based on the *in situ* formation of reinforcing parameters inside the metal matrix significantly improve mechanical strength, hardness, and wear resistance of metal-based composites. Both techniques, ingot and powder metallurgy, can be used for producing the metal matrix composites reinforced with nano and microparticles, while the ingot procedures in most cases need to be combined with adequate heat treatment. The correlation between physical properties and phase transformation kinetics in copper-based alloy shows that the possibility for additional performance improvements exists.

Acknowledgments

This work is funded by the Ministry of Education, Science and Technological Development of the Republic of Serbia.

References

[1] D. Anderson, H. T. Michels: Metal Ions in Biology and Medicine, 10 (2008)185-190.
[2] T. R. Chen, P.Y. Lee: J. Mar. Sci. Technol. 1 (1993) 59-64.
[3] K. Sharvan Kumar, Development of dispersion-strengthened XD^{TM} Cu Alloys for high heat-flux applications, NASA Contractor report 191124, 1993.
[4] W. F. Smith, Structure and Properties of Engineering Alloys, second ed., McGraw Hill, New York, 1993.
[5] https://www.espimetals.com/index.php/technical-data/194-silver Accessed 01.09.2020.
[6] M. Š. Musa, Z. Schauperl: Process. Appl. Ceram., 7 (2013) 63–68.
[7] D. Chung, Applied Materials Science: Applications of Engineering Materials in Structural, Electronics, Thermal, and Other Industries / D.D.L., 2001.
[8] https://www.copper.org/resources/standards/uns-standard-designations.html Accessed 23. 08. 2020.
[9] J. Ružić, J. Stašić, S. Marković, K. Raić, D. Božić: Sci. Sinter. 46(2014) 217-224.
[10] J.S. Andrus, R. G. Gordon, NASA Contractor Report, Florida, 1989
[11] [R.S. Jankovskyet et al., NASA Technical Paper, Ohio, 1994

[12] H. Kimura, N. Muramatsu, K Suzuki, Copper Alloy and Copper Alloy Manufacturing
Method, US0211346A1, 2005.
[13] J. Stašić, M. Trtica, V. Rajkovic, J. Ružić, D. Božić: Applied surface science, 321 (2014) 353–357.
[14] A.K. Kuruvilla, K.S. Prasad, V.V. Bhanuprasad, Y.R. Mahajan: Scr. Metall. Mater., 24 (1990) 873–878.
[15] C. R. Wang, J. M. Yang, W. Hoffman: Mater. Chem. Phys. 74 (2002) 272–281.
[16] D. Božić, J. Stašić, B. Dimčić, M. Vilotijević, V. Rajković: Bull. Mater. Sci. 34 (2011) 217–226.
[17] C. R. Deckard, Method and apparatus for producing parts by selective sintering, Patent number WO 1988002677 A2, 1988.
[18] C. Wang, H. Lin, Z. Zhang, W. Li: J. Alloys Compd, 748 (2018) 546–552.
[19] M.M. Opeka, I.G. Talmy, E.J. Wuchina, J.A. Zaykoski, S.J. Causey: J. Eur. Ceram. Soc. 19 (1999) 2405.
[20] D. Božić, I. Cvijović-Alagić, B. Dimčić, J. Stašić, V. Rajković: Sci Sinter. 41 (2009) 143.
[21] C. Zou, Z. Chen, E. Guo, H. Kang, G. Fan, W. Wang, R. Li, S. Zhang, T. Wang: RSC Adv., 8 (2018) 30777.
[22] J.-C. Zhao, Methods for Phase Determination, first ed. Ge Global Research, New York, 2007.
[23] J.-C. Zhao, M.R. Notis, J. Phase Equilib. 14 (1993) 303.
[24] J.-C. Zhao, M.R. Notis, Acta Mater. 46 (1998) 4203.
[25] P. B. Fernandes, G. C. Coelho, F. Ferreira, C. A. Nunes, B. Sundman: Intermetallics 10 (2002) 993.
[26] J.-C. Zhao, M.R. Jackson, L.A. Peluso: Acta Mater. 51 (2003) 6395.
[27] M. Li, L. Zhang, M. Zhu, Physical Properties and Precipitate Microstructures of Cu-Hf
Alloys at Different Processing Stages, Hindawi, 2018
[28] T. Rongzhang, W. Zhutang, Copper Alloy and Its Processing Manual, Central South University Press, 2002.
[29] D. Shangina, Y. Maksimenkova, N. Bochvar et al.: Open J. Adv. Mater. Res. 922 (2014) 651–656.
[30] D. V. Shangina, J. Gubicza, E. Dodony et al.: J. Mater. Sci. 49 (2014) 6674–6681.

CreativeCommonsLicense

This work is licensed under a Creative Commons Attribution 4.0 International License.